Rapid, High Resolution Probe Screening Techniques for Core Analysis and their Potential Usefulness for Hydrocarbon or Energy Transition Applications

Emmanuel Okwoli and *David K.* Potter*

Department of Physics, University of Alberta, Edmonton, Alberta, T6G 2E1, Canada

Abstract. Core analysis techniques have traditionally been used mainly for hydrocarbon reservoir applications. However, the same techniques are equally applicable to reservoir issues associated with energy transition, such as geothermal, carbon geosequestration and hydrogen storage. Traditionally much core analysis has been performed successfully using core plugs. However this approach has certain drawbacks: (1) the selected plugs may not necessarily be representative of the full range of lithologies, (2) key features (e.g., naturally cemented or fractured zones) may be missed, (3) high resolution detail at the lamina scale may be missed, (4) depth shifting to well logs may not be sufficiently accurate, and (5) this strategy may be more sensitive to missing core. In this paper we highlight the usefulness of probe core analysis techniques on slabbed core and powdered samples. For many reservoirs relevant to energy transition it is crucial to have a high resolution continuous record of petrophysical properties so that key features are not missed (e.g., seals and fractures that may be important for CO_2 or H_2 storage applications). Probe measurements are less-destructive, without the need to cut core plugs, and provide: (1) high resolution data at the lamina scale, so that key features and small scale heterogeneities can be identified, (2) improved depth matching to well log data, and (3) rapid, cost effective data. In this paper we will describe examples highlighting a number of different probe techniques. Whilst some are well known, such as probe permeability, others such as probe acoustics, probe luminance (from linear X-ray measurements) and probe magnetics are less familiar to core analysts, but are very well suited for analyzing cores from reservoirs associated with hydrocarbons and energy transition. For example, certain geothermal projects will involve studying igneous as well as sedimentary rock cores, and differences in the magnetic susceptibility signals using the small, portable magnetic probe can quickly differentiate the higher signals of the igneous samples from the much lower values of the sedimentary rocks. The acoustic probe can be used to: (1) rapidly identify anisotropy (by orienting the acoustic transmitter-receiver bracket in different directions), (2) identify open microfractures via longer transit times, and (3) produce high resolution porosity profiles (after correlation of transit times with some representative plug or well log porosity data). Probe luminance and associated linear X-ray images, which are related to density, can indicate the full extent of natural cemented zones that may not be seen from mere visual observations of the slabbed core surface.

1 Introduction

The most common laboratory petrophysical analysis technique has been to cut and analyze cylindrical core plugs [1-3]. Core plugs are useful for characterizing 3D properties, and for simulating reservoir conditions through pressure and temperature experiments, and have yielded important information for formation evaluation and reservoir characterization (e.g., [4,5]) However, there remain some limitations of traditional core plug analyses and their sampling strategies:

(i) Cutting routine core plugs every 1 foot along the whole core sample is expensive and time-consuming and more destructive to core than probe measurements on slabbed core.

(ii) Depth shifting to well logs may not be sufficiently accurate even when cutting plugs every 1 foot.

(iii) This sampling strategy is sensitive to missing core.

(iv) The selected plugs might not represent the full range of lithologies or features. For instance, vital geologic features such as thin, naturally cemented zones that could act as permeability seals (i.e., barriers to fluid flow) may be missed.

Therefore, in this present study, we analyzed some datasets comprising novel probe measurements undertaken mainly on slabbed cores (though in one case powdered samples). Slabbed core creates a flat surface that allows probe measurements to conveniently be taken

* Corresponding author: dkpotter@ualberta.ca

at high resolution along the core. These probe high resolution and less-destructive screening techniques have advantages over the conventional 1 core plug per foot sampling strategy as follows:

(i) They allow high resolution measurements (at the small lamina scale) to be undertaken, so that key features and small scale heterogeneities can be identified. For example, identifying naturally cemented zones comprised of barite or quartz overgrowths. The high resolution profiles also allow better depth matching to well log data.

(ii) They are rapid screening methods, thus saving time by allowing quick petrophysical appraisals of the core samples to be made long before the routine or special core analysis plug data becomes available.

(iii) They are less-destructive, which is particularly useful for unconsolidated samples such as oil sands.

(iv) They do not require any special preparation of the sample. Some other core laboratory techniques require significant sample preparation. For example, laboratory nuclear magnetic resonance (NMR) generally requires the sample to be saturated with an appropriate fluid.

This paper will first describe a variety of probe techniques, some of which may be less familiar to core analysts. The advantages of probe permeability profiling (rapid, high resolution measurements) on slabbed core have been recognized for some time [6]. More recent studies have related probe permeability measurements to fluid flow and hardness in selected formations in western Canada [7], and modelling the effect of anisotropy on probe permeability [8]. Whilst there has been a recent study applying a new linear X-ray technique to measure the attenuation coefficients of various materials such as plastic, plexiglas, silicone rubber and paraffin wax [9], linear X-ray and quantitative point X-ray (probe luminance) measurements on rocks have received little attention since the work of Duncan et al [10]. Likewise there is little mention of probe acoustics techniques in the literature. We have, however, conducted recent studies using a probe magnetic device for characterizing some turbidite, shale and oil sands samples [11, 12]. In this paper we will present some examples of the usefulness of each of the above mentioned probe techniques, which can be applicable not only for hydrocarbon reservoir analyses but also for reservoirs associated with energy transition.

2 Experimental Probe Methods

2.1 Linear X-ray Images and Quantitative Point X-ray (Probe Luminance)

A schematic of the linear X-ray experimental setup is shown in **Figure 1** (after [10]). X-rays from the source pass through the rock sample and create an inverted image on an electronic image intensifier. The visible image is picked up by a charge coupled device (CCD) camera and digitized. The image can be viewed in real time and approximately 6-7 inches (roughly 15-18 cm) of rock core can be observed at any one time within the camera frame. The frames can be combined to produce composite images (about 3 ft or 1 m in length in the present study). Overlaps of roughly 1 inch between neighbouring frames are utilized to achieve optimum matching in the composite image.

Typically, 3 ft lengths of cylindrical whole core with a diameter of 4 inches (just over 10 cm) are analyzed. Slabbed core can also be analyzed or, alternatively, a slice from the whole core of constant thickness (about 0.4 inches or 1 cm) can be used. Such slices are often impregnated with resin and referred to as resinated slabs. In parts of the core where there may be no rock, for example when a small core plug has been cut and removed from the larger core sample, the X-ray image appears very bright (white). This is the result of saturation or burn out within the image intensifier, due to the higher intensity of X-rays where there is no rock to block them.

The digital X-ray images are composed of pixels of varying gray scale (arbitrarily set between 0 and 255). The gray scale, known as the luminance, can be read in real time at any point across the image. By taking regularly spaced point readings (about every 0.032 ft or 1 cm in the current study) a quantitative high resolution profile of gray scale variation can be produced along the core sample, which in the present study will be referred to as “probe” luminance data. The luminance values represent the penetrability of the rock core to X-rays and are inversely related to the density of the rock [10]. Higher luminance values (lighter images) represent lower density, whilst lower luminance values (darker images) represent higher density.

The point probe luminance values (averaged over an area of about 0.5 cm diameter) can be taken in just a few seconds and are dependent on the thickness of the rock sample. To ensure all results in the present study were obtained from a similar thickness of slabbed core the luminance measurements were taken along the central axial line of the slabbed core, which had a constant thickness of 2 inches (just over 5 cm). This ensured that true variations in density could be identified without needing to correct for changes in core thickness. Also, in the absence of any independent bulk density data (which could otherwise be used to correlate with the luminance values) an aluminium block calibration standard of known density can be placed at the top and bottom of each 3 ft section and its luminance value measured in order to help produce density data for the rock core from the rock’s luminance results.

2.2 Probe Magnetic Susceptibility

Magnetic susceptibility is usually expressed in terms of magnetic susceptibility per unit volume k as:

$$k = J/H \qquad (1)$$

or in terms of magnetic susceptibility per unit mass χ as:

$$\chi = M/H = k/\rho \qquad (2)$$

where J is the magnetization per unit volume, M is the magnetization per unit mass, H is the applied external magnetic field, and ρ is the density of the material. A Bartington MS2E probe sensor can be used to perform high resolution measurements of magnetic susceptibility along the flat surface of slabbed core, or on individual smaller samples, or powdered rock samples. We have used this type of sensor for some other recent reservoir analyses on consolidated, unconsolidated, conventional and unconventional samples [11, 12]. However, all our previous studies were related to sedimentary reservoirs. We will show an example here of the use of this sensor in a potential geothermal setting where one encounters not only sedimentary samples, but also igneous core samples. The sensor tip at the end of a ceramic tube (label **1** in **Figure 2 (A)** and label **4** in **Figure 2 (B)**) senses a rectangular surface area of 3.8 mm x 10.5 mm on the sample. This allows high resolution measurements to be made at the lamina scale. The sensor is calibrated to measure true volume magnetic susceptibility (k) when against a flat surface of a sample greater than 10 mm in thickness. Most of the magnetic susceptibility signal is acquired within a penetration depth of up to about 5 mm into the sample. The ceramic tube is mounted on a metal enclosure that houses the electronic circuitry. When the sensor is connected to the MS2 meter (**Figure 2 (C)**) via a cable and the power is supplied, a low intensity alternating field (about 80 Am^{-1} and about 2 kHz in frequency) is generated. This applied field penetrates a few mm into the sample when the tip of the sensor is gently placed on the flat surface of the slabbed core or individual sample. For samples with a weak magnetic susceptibility signal, such as the majority of sedimentary rocks, a background reading (in 12 seconds) followed by the sample measurement (in 12 seconds) can be made on the sensitive setting. For strong magnetic susceptibility samples, such as igneous and metamorphic rocks, each measurement can be made in just 1 second on the less sensitive setting. Another small sensor connected to a furnace (**Figure 2 (D)**) can make magnetic susceptibility measurements at different temperatures so that, for example, the effects of borehole temperatures can be simulated.

2.3 Pressure Decay Probe Permeametry

The experimental setup for the probe permeability measurements is shown in the photo of **Figure 3** and the schematic of **Figure 4 (a).** In the example we show in the results **section 3.2** a Core Laboratories PDPK-400 unsteady state pressure decay probe permeameter was used to take point readings at exactly the same points along the slabbed core where the probe luminance values were taken. The tank shown in **Figures 3** and **4a** is first filled with nitrogen gas to a pre-defined pressure, and the valve closed. The probe tip is then sealed onto the core sample (in this case the surface of the slabbed core). A small probe tip of internal diameter 0.524 cm was used in the present study, which was comparable to the area of the point luminance measurements. The valve is then opened and the decay of pressure with time is recorded. After some time, a smooth pressure gradient is established in the sample. The slope of the pressure decay curve is equal to the instantaneous flow rate function. This type of probe permeameter generally gives readings faster than the older steady state permeameters, which require one to wait for an equilibrium position to be reached at which the pressure and flow rate are constant. The permeameter delivers the permeability value of highly permeable rocks in a few seconds, whilst the value of low permeability rocks may take several minutes since the nitrogen gas will take longer to penetrate into the sample.

2.4 Probe Acoustics

The Core Laboratories PDPK-400 permeameter also enables the probe tip to be replaced with a small acoustics bracket (a simplified schematic is shown in **Figure 4 (b)**) to allow rapid, high resolution acoustic measurements of *p*- and *s*-wave transit times to be made on core samples. The bracket consists of two pyramidal point transducers (essentially two upside down pyramids separated by a distance of just under 10 cm), one being the transmitter (producing an acoustic pulse at a frequency of 1 MHz) and the other the receiver. The acoustic pulse penetrates just a few millimetres into the surface of the core, and measures the transit time (which can be converted to a velocity) over the interval between the transducers on the slabbed core. One advantage of these measurements is that the bracket can be rotated to make measurements in different orientations in order to gain information on the acoustic anisotropies of the different rock lithologies. In the present study we have measurements taken in two orthogonal directions, horizontally and vertically along the slabbed core surface. For the horizontal or vertical measurements, the mid-point of the acoustic bracket was placed over the points at which the luminance and probe permeability measurements were taken. Another advantage of the acoustic measurements is that by calibrating with a few core porosity measurements one can estimate porosity values from the probe acoustic results, and thus provide a high resolution "probe porosity" profile along each slabbed core section.

3 Results and discussion

3.1 An example of the usefulness of linear X-ray and probe luminance measurements

Figure 5 shows an example of the additional information that can be acquired from linear X-ray and luminance measurements. The slabbed core visible light image in **Figure 5 (a)** shows the presence of a very thin naturally cemented fracture vein containing barite ($BaSO_4$). Almost all the barite filled fracture veins observed in this well (in the North Sea) appeared very thin and of limited extent on the flat surface of the slabbed core in visible light. However, linear X-ray images such as that in **Figure 5 (b)** showed that most of these barite filled fracture zones were much more

extensive in 3D. Many of them exhibited a dendritic pattern with a thicker "trunk" region and thinner "branches" at right angles to the "trunk." It is important to know the true extent of these barite filled fracture veins either in cases where you may want a good seal (e.g., for CO_2 or H_2 storage applications), or in cases where you don't want a low permeability sealing interval. Relying only on visible light images of the core may not necessarily identify the full 3D extent of these natural cemented features.

Figure 6 shows that the luminance values from the linear X-ray images of **Figure 5 (b)** correlate reasonably well with the borehole bulk density log values. The smoothed luminance values in this case are 7 point running vertical averages over 1.5 ft intervals. This interval size was taken to compare directly with the vertical interval over which the wireline bulk density log averaged each reading.

3.2 An example of a comparison between probe luminance, probe permeability and probe acoustics

Figure 7 shows the raw probe measurement profiles (probe luminance, probe permeability and probe acoustic transit times for the *p*-waves) with depth for a 36 ft slabbed core interval from a well in the North Sea. **Figure 7** also shows the different lithological units within this interval of interest. These comprise the main good reservoir unit (white sections), which is a quartz sandstone shoreface facies intercalated with clay, a calcite dogger (yellow sections) comprising calcite and clays, and a micaceous sandstone (green section). Note that the depths are merely the depths from the top of the interval studied (as the real depths are confidential). The best reservoir (white sections) is part of the Etive formation in the North Sea. The micaceous sandstone (green section) is still reservoir, but of lower quality, and is part of the Rannoch formation in the North Sea. The calcite doggers (yellow sections) are essentially natural cemented zones with very low porosity and permeability.

Figure 7 shows quite similar overall profiles with depth for the probe luminance and probe permeability. Both are low in the calcite dogger sections, generally higher in the good reservoir Etive formation, and generally lower again in the lower quality Rannoch formation. Higher values of probe luminance and probe permeability in the Etive tend to be pure quartz sandstone with little clay, whereas lower values in the Etive are generally associated with intercalated clay laminae. The probe acoustic transit times follow a generally similar overall pattern as the other probe results, being lower in the calcite doggers and Rannoch micaceous sandstone and higher in the Etive reservoir. Two sets of probe acoustic results are shown: one set where the acoustic bracket made measurements horizontally down the slabbed core, and another set where the acoustic bracket made measurements vertically down the slabbed core. There is a significant difference between the horizontal and vertical probe acoustic measurements in the Rannoch micaceous sandstone. This is due to anisotropy caused by the small mica flakes that aligned along the bedding plane (the ancient horizontal) when the rock formed, causing the transit time to be lower in the horizontal (higher velocity) and longer in the vertical direction (lower velocity). Detecting this anisotropy from these rapid measurements is very useful, particularly since the standard sonic log for this well only measured the transit time over vertical intervals (as is the case for many wells), and gave a profile close to that of the vertical probe acoustics. Thus the standard sonic log data would not have identified the anisotropy.

In the Etive reservoir sections there are some zones where the horizontal and vertical probe acoustic results are very similar. These represent zones that are close to being isotropic and correspond to clean quartz sandstone zones (i.e., where there is little or no clay). There are other parts of the Etive reservoir where the horizontal and vertical probe acoustic results are very different. These represent anisotropic zones where the quartz sandstone is intercalated with thin clay laminae.

To compare the different petrophysical probe parameter results, we first crossplotted the raw data points and observed correlations, though the coefficients of determination (R^2) were relatively low. This could be due to small differences in depth matching of the crossplotted parameters. The raw data points for different parameters need to be very accurately matched to exactly the same depth (which can be quite challenging) for good correlations to be observed. We then crossplotted smoothed data over different vertical running averages (1 ft, 1.5 ft, and 2 ft). The smoothed data averages the results over a particular interval and so any small inaccuracies in depth matching will have minimal effect since most of each interval will match for both parameters concerned. Another reason for smoothing the data was because the acoustic probe measures the transit time over an interval of just under 10 cm (and is thus an average over this interval rather than being a point measurement), whereas the probe permeability and probe luminance are essentially point measurements over a small area (as detailed in the experimental methods **section 2**). Therefore, it was logical to compare all of the probe results by using a running average (i.e., smoothing). The vertical acoustic measurements, in particular, were often taken across different thin laminae and fractured sections, so it was important to average the other point probe measurements across the same intervals. The smoothing significantly improved the coefficient of determination (R^2) values, with the highest R^2 values obtained when averaging over a 2 ft vertical interval. The correlation between probe luminance and probe permeability gave an R^2 value of 0.48 when comparing the raw data points and a much improved R^2 value of 0.76 when the smoothed 2 ft vertically averaged data was crossplotted. For the vertical probe acoustics versus probe permeability, an R^2 value of 0.41 was obtained for the raw data, and an R^2 value of 0.85 for the data averaged vertically over 2 ft intervals. For the horizontal probe acoustics versus probe permeability the R^2 value was only 0.37 for the data averaged vertically over 2 ft intervals (and lower for the

raw data crossplot). This was mainly due to lower correspondence in the top calcite dogger interval (the reason is not clear at present). However, there was good correspondence throughout the rest of the 36 ft interval. Moreover the horizontal acoustics correlated with permeability better than the vertical acoustics in the micaceous sandstone interval. We believe this was a result of the anisotropy. Both the horizontal acoustics and probe permeability essentially measured in the horizontal plane of the mica grains, whereas the vertical acoustics measured perpendicular to that plane. For the vertical probe acoustics and probe luminance measurements, an initial R^2 value of 0.51 was obtained for the raw data, and a value of 0.70 for the data averaged vertically over 2 ft intervals. More extensive comparative analyses of this large dataset, involving multiple linear regression and artificial neural networks, is being prepared for publication elsewhere.

Figure 8 shows another example from this dataset of the usefulness probe permeability measurements. It shows the same probe permeability profile as in **Figure 7**, but also shows the core plug permeability values for comparison. One observation is that the core plug values tend to be higher on average than the probe values at corresponding depths. We believe this is because the core plugs were cleaned by hot soxhlet cleaning, and some of the permeability controlling clays are likely to have been washed out of the samples prior to the permeability measurements. This would have led to higher permeability values than for the uncleaned slabbed core with the original clay content. We have previously quantified the removal of clay in other core plug samples using magnetic susceptibility measurements before and after cleaning [13].

Figure 8 also shows that the probe permeability values exhibit much more detail, due to the higher measurement resolution (at the lamina scale), and a much larger range of values compared to the core plugs. This level of detail can be crucial for identifying thin naturally cemented zones, or thin open fractures, or thin laminae (which could be low permeability seals or high permeability conduits), not only in hydrocarbon reservoirs but also in potential reservoirs for CO_2 or H_2 storage. Sampling of core plugs tends to avoid some of features. This may also partly explain the smaller range of plug permeability values compared to the probe permeability values in **Figure 8**.

3.3 Probe magnetic susceptibility measurements on samples from a pilot exploration well from a potential geothermal project in Northern Alberta

In Northern Alberta, the thickness of the Phanerozoic sedimentary succession is quite variable (between about 500 and 2400 m). Previous studies [14, 15] indicated that temperatures above about 80ºC for geothermal purposes will only be found below the base of sedimentary rocks in the Precambrian crystalline basement. Thus it is crucial to be able to identify the depths of the boundary between the sedimentary succession and the crystalline basement rocks. We proposed that magnetic susceptibility could easily identify the boundary between the sedimentary succession and the crystalline granitic basement rocks better than most other techniques. **Table 1** shows our probe volume magnetic susceptibility measurements for some test powdered samples from a deep pilot well to assess the viability of a geothermal project. The powdered samples were held in small plastic containers (about 1 cubic inch in volume), which were open at one end, allowing the probe magnetic susceptibility device to be gently placed on the top surface of each powdered sample to take the measurements. Sample H22 is still part of the sedimentary succession (but may possibly be slightly metamorphosed) and has a low volume magnetic susceptibility. Samples H25 and H28 are within the crystalline granitic basement and have significantly higher volume magnetic susceptibility values. It thus appears that magnetic susceptibility is a good means of identifying the depth at which the crystalline basement starts. The compositions of the samples, from electron microprobe data and whole rock geochemistry, are given in **Table 2**. However, it is not these major components listed in **Table 2** that are primarily responsible for the large differences in magnetic susceptibility between the sediment sample and the two basement samples. It turns out that the small fraction of ferrimagnetic iron oxides in the samples is the key factor. Whilst the sediment sample contains an extremely small amount of stable single domain ferrimagnetic particles (which we identified from magnetic hysteresis measurements similar to those described in [16]) that don't increase the overall magnetic susceptibility of the sample significantly, the two crystalline basement samples contain small amounts of superparamagnetic ferrimagnetic particles (also identified from magnetic hysteresis measurements) that do contribute significantly to the higher magnetic susceptibility of these samples.

3.4 Summary of the probe techniques and examples of hydrocarbon and energy transition applications

Table 3 summarizes the different probe techniques described in this paper, and lists of some of the potential significant/relevant applications to hydrocarbon and energy transition studies. The probe luminance and probe permeability measurements are essentially point readings over small (very similar diameter) areal extents, as detailed in **sections 2.1 and 2.3**, and can give data at the lamina (a few millimetres) scale. The probe magnetic susceptibility measurements are also essentially a point reading, but over a slightly larger rectangular areal extent and also at the lamina (a few millimetres scale) as detailed in **section 2.2**. The probe acoustics tool gives a transit time over an interval of just under 10 cm as detailed in **section 2.4**, and will give the transit time of individual thin laminae if the transducer bracket is placed parallel to the laminae, and may give an average value of a number of laminae if the transducer bracket is placed perpendicular to laminae that are thinner than the distance between the transmitter and receiver transducers.

4 Conclusions

The following overall conclusions can be drawn:

1. Probe measurements have the potential to provide rapid, high resolution, less destructive measurements compared to core plugs, and provide additional complementary tools for analyzing reservoir samples for hydrocarbons or energy transition (e.g., CO_2 and H_2 storage, and geothermal applications).

2. Linear X-ray measurements allow one to see the full 3D extent of features such as naturally cemented zones (e.g., barite filled fracture veins). Probe luminance values can be used to provide a high resolution profile of density variation, and can be correlated with other probe petrophysical techniques (such as probe permeability and probe acoustics).

3. Probe permeability can rapidly characterize variations at high resolution (at the lamina scale) on slabbed core. In contrast, routine core plug sampling strategies generally only cut plugs every 1 foot, and thus could miss certain key features (e.g., thin naturally cemented zones). Core plug cutting and analysis is also time consuming, and more destructive to the core. Also certain core cleaning processes such as hot soxhlet cleaning can potentially remove some permeability controlling clays, as quantified in our previous study [13]. This will subsequently produce overestimated permeability values, and is the likely reason for the high core plug permeability values compared to the probe permeability values in the example we give in the present paper in **Figure 8**.

4. Probe acoustic measurements taken in different orientations can quickly identify and quantify anisotropy (of acoustic transit time) in different lithologies. This can be particularly useful if one only has access to standard sonic log data, which averages transit times over vertical intervals, and so wouldn't identify anisotropy.

5. Probe magnetic susceptibility measurements can rapidly distinguish sedimentary from crystalline granitic basement samples for geothermal applications. This is in addition to other applications of probe magnetic susceptibility (e.g., for turbidites, shales, and oil sands) that we have described previously [11, 12].

D. K. P. thanks the Natural Sciences and Engineering Research Council of Canada (NSERC) for a Discovery Grant. We thank Core Laboratories for their help with the probe permeability and probe acoustic measurements, and Corex (formerly Robertson Research) for their help with the linear X-ray and luminance measurements. Olga Vizika and Subhash Ayirala are thanked for their constructive review comments, which helped improve the manuscript.

5 References

1. A. Donaldson and G. M. Clydesdale. Accurate reservoir evaluation – quality core samples – a good starting point. *In: Advances in Core Evaluation – Accuracy and Precision in Reserves Estimation (Ed. P.F. Worthington),* p. 35–53. Gordon & Breach Science, New York (1990)
2. B. Levallois. Core petrophysical measurements on unconsolidated sands in deep water reservoirs. *Proceedings of the 2000 International Symposium of the Society of Core Analysts, Abu Dhabi, UAE, 18-20 October,* Paper SCA2000-34 (2000)
3. C. E. Ubani, B. Y. Adeboye and B. A. Oriji. Advances in coring and core analysis for reservoir formation evaluation. Petroleum & Coal, **54**, 1-15 (2012)
4. T. A. Zorski, J. S. Ossowski, N. Rodo and T. Kawiak. Evaluation of mineral composition and petrophysical parameters by the integration of core analysis data and wireline well log data: The Carpathian Fore deep case study. Clay Minerals, **46** (1), 25–45 (2011)
5. H. M. Sbiga and D. K. Potter. Prediction of resistivity index by use of neural networks with different combinations of wireline logs and minimal core data. SPE Reservoir Eval. Eng. **20** (1), 240–250 (2017) https://doi.org/10.2118/181751-PA.
6. D. J. Goggin. Probe permeametry: is it worth the effort? Marine and Petroleum Geology, **10**, Issue 4, 299-308 (1993)
7. C. P. Vocke, C. R. Clarkson, S. Aquino, A. Vahedian, D. C. Lawton, K. Osadetz and A. Ghanizadeh. Application of profile (probe) permeability and mechanical (rebound) hardness tests for characterization of fluid transport and geomechanical properties of selected formations in western Canada. *GeoConvention 2016: Optimizing Resources*, *Calgary*, (2016)
8. K. Al-Azani, H. Al-Yousef and M. Mahmoud. Effect of permeability anisotropy on probe permeameter measurements. *SPE Middle East Oil and Gas Show and Conference, Manama, Bahrain*, Paper SPE-194769-MS (2019)
9. A. Mousa, K. Kusminarto and G. B. Suparta. A new simple method to measure the X-ray linear attenuation coefficients of materials using micro-digital radiography machine. International Journal of Applied Engineering Research, **12**, number 21, 10589-10594 (2017)
10. A. R. Duncan, G. Dean and D. A. L. Collins. Quantitative density measurements from X-ray radiometry. *In: Harvey, P. K. and Lovell, M. A. (eds) Core-Log Integration,* Geological Society, London, Special Publications, **136**, 17-24 (1998)
11. T. H. To, D. K. Potter, A. Abiola, and V. T. Ebufegha. Probe magnetics as a rapid, non-destructive screening tool for consolidated and unconsolidated core in conventional and unconventional reservoirs. *Proceedings of the 2018 International Symposium of the Society of Core*

Analysts, 27-30 August 2018, Trondheim, Norway. Paper SCA 2018-057 (2018)
12. T. H. To and D. K. Potter. Comparison of high resolution probe magnetics, X-ray fluorescence and permeability on core with borehole spectral gamma ray and spontaneous potential in an oil sand well. *Proceedings of the 34th International Symposium of the Society of Core Analysts*, Paper SCA2021-035, (2021)
13. D. K. Potter, A. Ali, S. Imhmed and N. Schleifer. Quantifying the effects of core cleaning, core flooding and fines migration using sensitive magnetic techniques : implications for permeability determination and formation damage. Petrophysics, 52 (no. 6), 444-451 (2011)
14. F. W. Jones, H. L. Lam and J. A. Majorowicz. Temperature distributions at the Paleozoic and Precambrian surfaces and their implications for geothermal energy recovery in Alberta. Canadian Journal of Earth Sciences, **22**, 1774-1780 (1985)
15. J. Majorowicz, M. Unsworth, T. Chacko, A. Gray, L. Heaman, D. K. Potter, D. Schmitt and T. Babadagli. Geothermal energy as a source of heat for oil sands processing in Northern Alberta, Canada. In : F. J. Hein, D. Leckie, S. Larter and J. Suter, eds., Heavy-oil and oil sand petroleum systems in Alberta and beyond. AAPG Studies in Geology, **64**, 1-22 (2012)
16. O. P. Ivakhnenko and D. K. Potter. The use of magnetic hysteresis and remanence measurements for rapidly and non-destructively characterizing reservoir rocks and fluids. Petrophysics, **49**, (issue 1), 47-56 (2008)

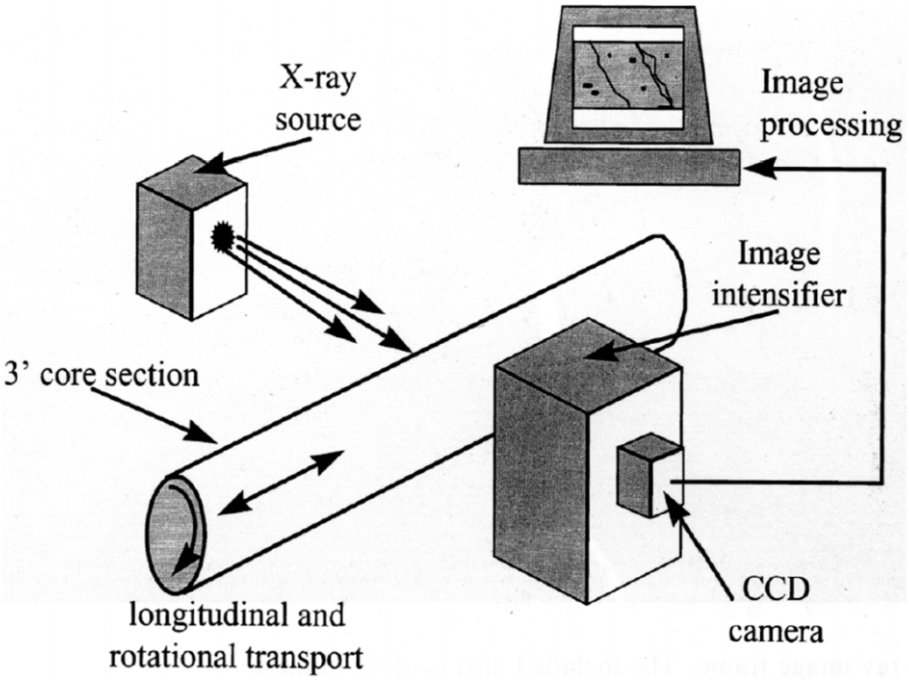

Fig. 1. Schematic of the equipment for linear X-ray and probe luminance measurements (after [10]).

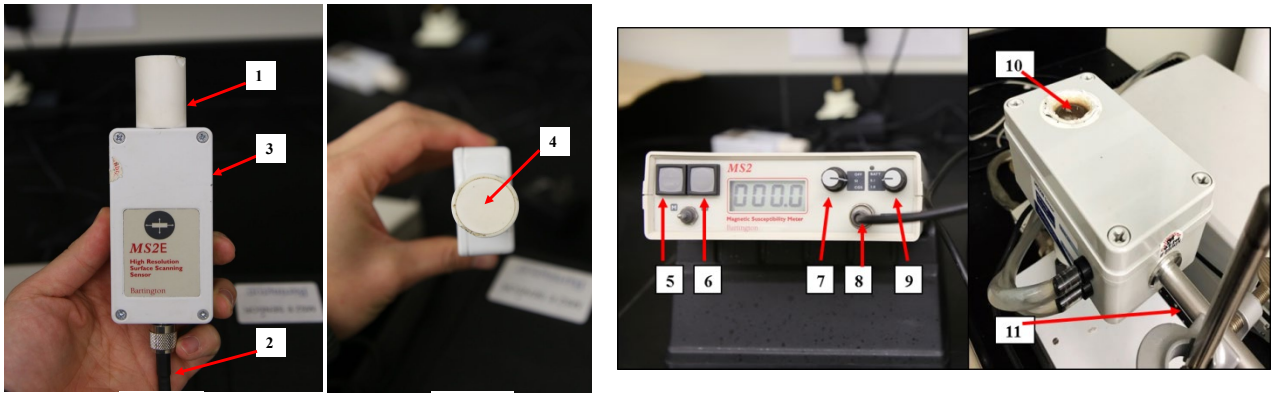

(A) **(B)** **(C)** **(D)**

Fig. 2. MS2E probe for magnetic susceptibility measurements on slabbed core. **(A)** side view showing: **1** the probe tip with a ceramic guard and a sensor located at the end of the tube, **2** the cable connected to the MS2 meter, **3** a metal enclosure housing the electronic circuity. **(B)** top view **4** shows the cross section of the probe sensor tip that is gently applied to the surface of the slabbed cores. **(C)** View of the magnetic susceptibility meter showing: **5** the measuring button, **6** the zeroing button, **7** is the magnetic unit (SI or CGS) system selector knob, **8** the cable connecting the MS2 meter to the sensor, **9** the sensitivity scale selector knob. The digital readout between **6** and **7** records the magnetic susceptibility value. **(D)** is the MS2W sensor for temperature dependent measurements (e.g., to simulate borehole temperatures) where **10** is the sample chamber and **11** is the input for the cable **8** shown in **(C)** to connect with the meter.

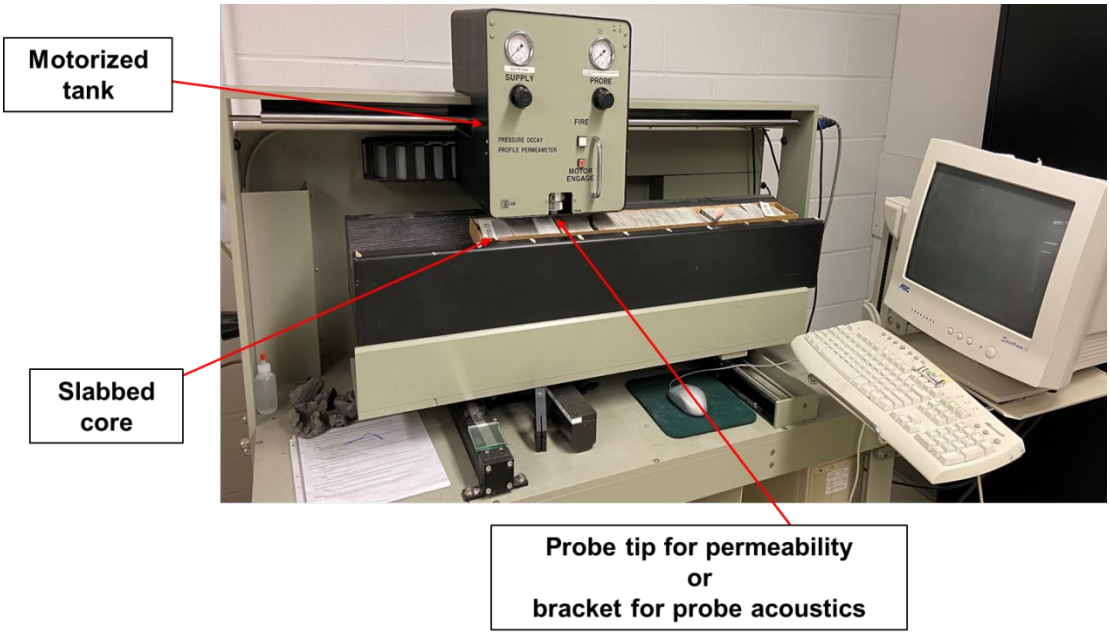

Fig. 3. Core laboratories PDPK-400 for probe permeametry and probe acoustics.

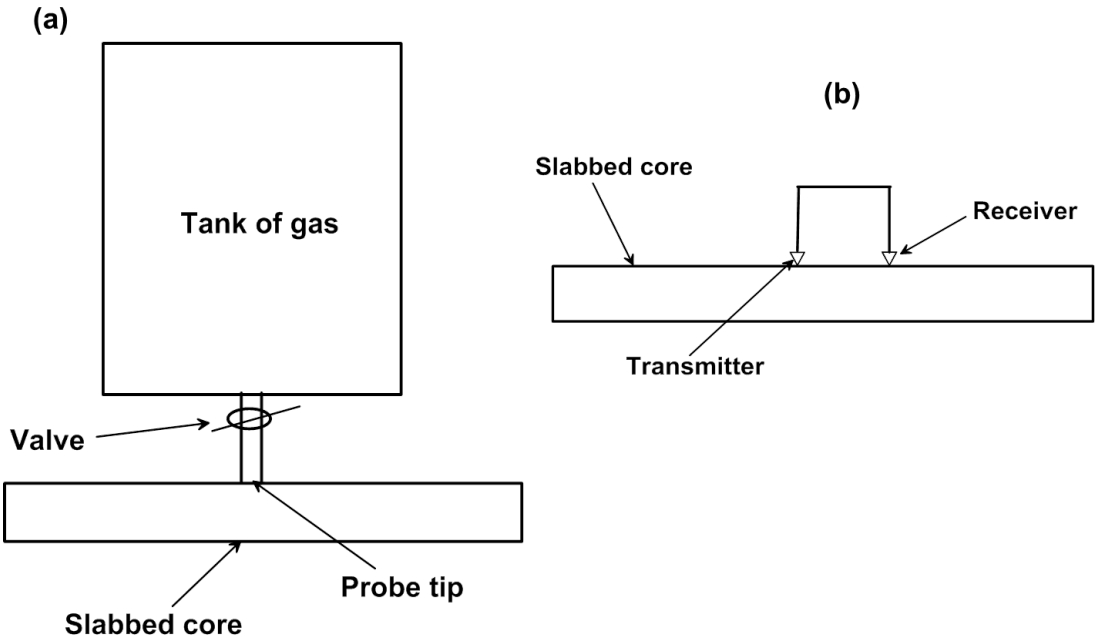

Fig. 4. Schematics of (a) the probe permeameter, and (b) the acoustic transducers.

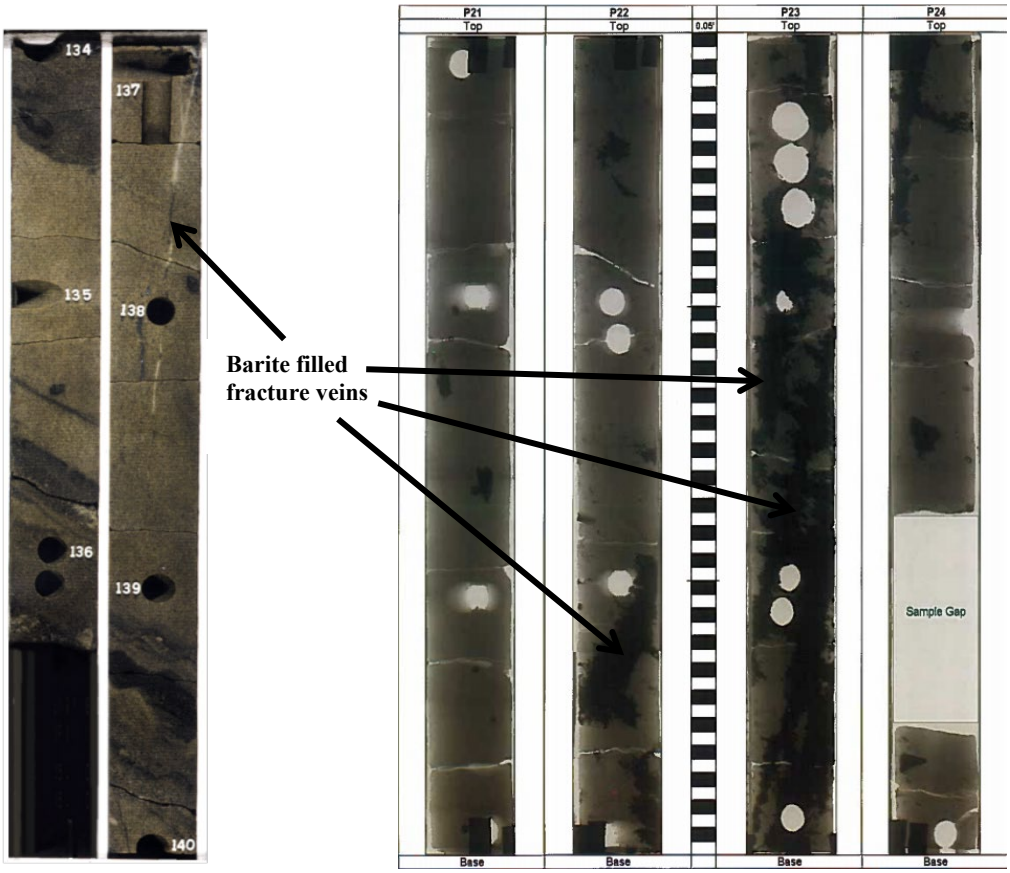

Fig. 5. (a) Visible light image of part of the slabbed core from a well in the North Sea, showing a thin barite filled fracture vein. The width of the core is 4 inches. **(b)** Linear X-ray images of core from the same well as in **(a)** showing that the barite filled fracture veins (black regions) are more extensive in linear X-ray than they appear in visible light. The lighter grey regions are quartz sandstone.

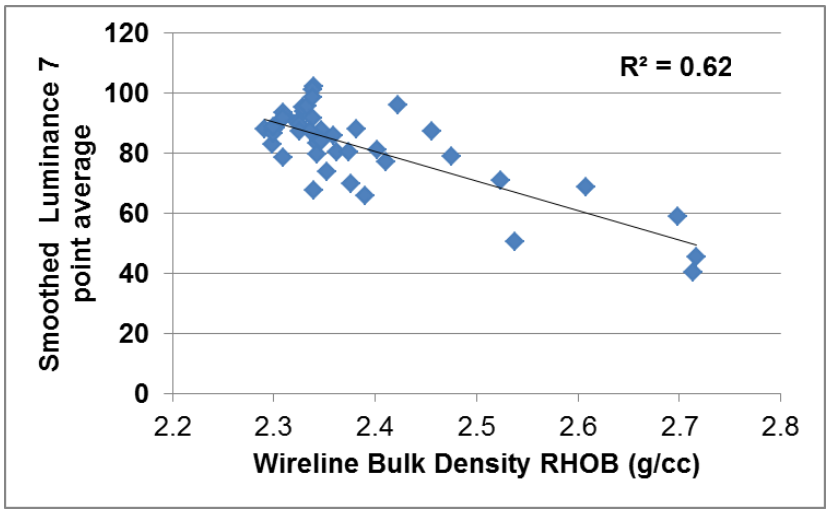

Fig. 6. Crossplot of wireline bulk density versus smoothed luminance 7 point average (averaged over 1.5 feet vertically) for the interval shown in **Figure 5 (b)**.

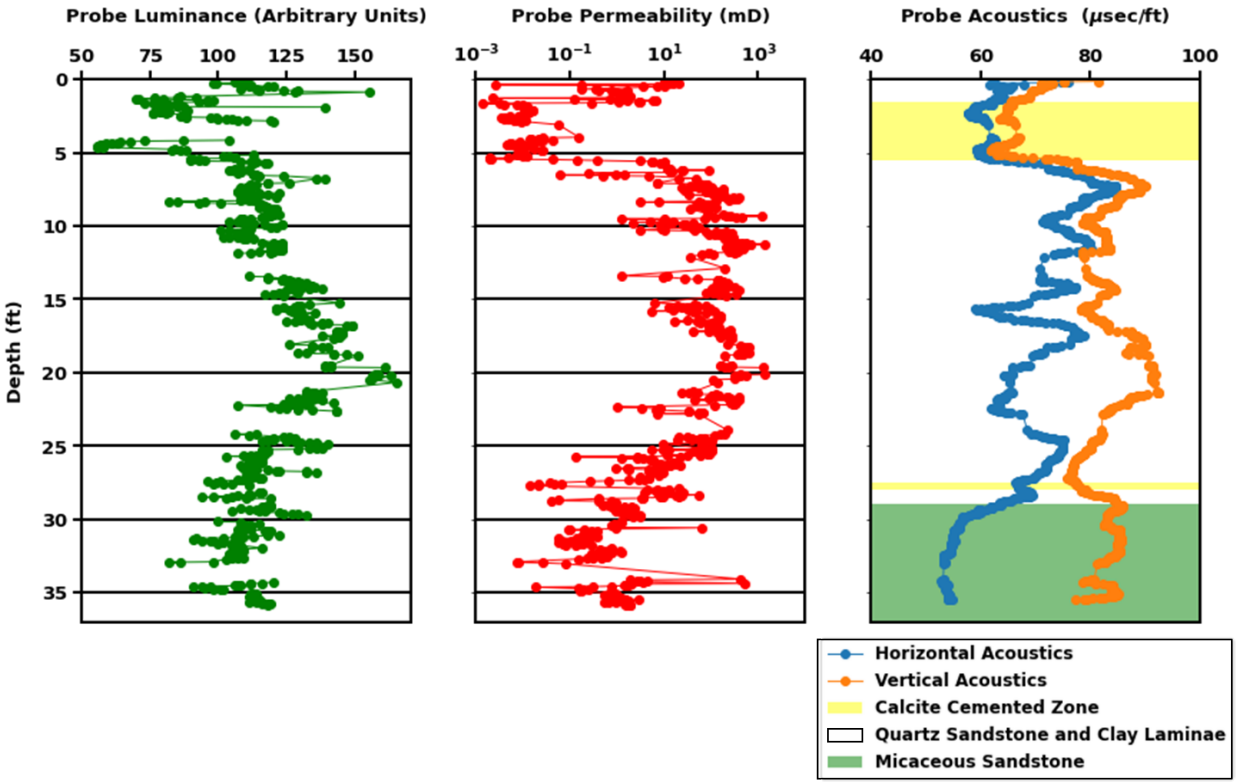

Fig. 7. Lithology and the variation with depth of **(left)** probe luminance **(middle)** probe permeability and **(right)** probe acoustic *p*-wave transit time measurements, for a well in the North Sea. The measurement uncertainties in each case are smaller than the plotted symbols. Typical uncertainties are as follows: for probe luminance ± 1; for probe permeability it depends somewhat on the magnitude being typically around ± 0.01 mD for permeabilities of 1 mD and around ± 10 mD for permeabilities of 1000 mD; for probe acoustics ± 1μsec/ft.

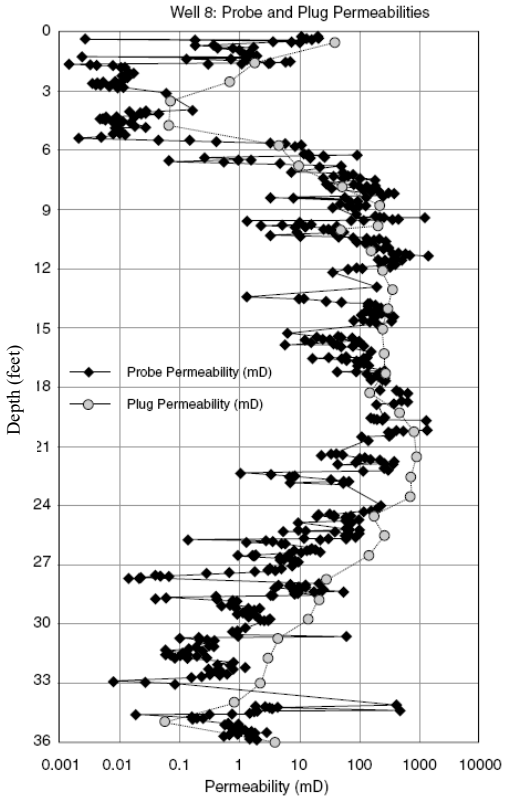

Fig. 8. Plot of the probe permeability values from **Figure 7**, and also showing the core plug permeability values for comparison.

Table 1. Low field probe volume magnetic susceptibility measurements on three powdered rock samples from a Well in Northern Alberta that is part of a pilot geothermal project study. The low field measurements were taken with a Bartington MS2E sensor. The sediment sample is clearly distinguished from the two crystalline basement samples on the basis of the magnetic susceptibility.

Sample name	**Sample depth (m)**	**Low field probe volume magnetic susceptibility at room temperature (10^{-5} SI)**
H22 (sediment)	1657	19
H25 (crystalline basement)	2350	506
H28 (crystalline basement)	2364	239

Table 2. Major components of the three powdered rock samples from **Table 1** from electron microprobe data and whole rock geochemistry.

Sample	**Quartz (%)**	**K-feldspar (%)**	**Plagioclase (%)**	**Orthopyroxene (%)**	**Other (%)**
H22 (sediment)	52	4	32	0	12 (mainly biotite)
H25 (crystalline basement)	25	13	53	6	3
H28 (crystalline basement)	28	13	50	6	3

Table 3. Summary of the probe techniques and some examples of their significance/relevance to hydrocarbon and energy transition applications.

Probe Technique	**Applications to Hydrocarbon and/or Energy Transition**
Probe Luminance	High resolution density, and identifying the 3D extent of naturally cemented intervals (important for reservoir seals for hydrocarbons, and for CO_2 and H_2 storage).
Probe Permeability	High resolution fluid flow, for identifying thin naturally cemented zones, open fractures, and laminae (which could be low permeability seals or high permeability conduits), for hydrocarbons, and for CO_2 or H_2 storage. Probe permeability measurements on uncleaned slabbed core do not suffer from clay removal caused by some cleaning processes on core plugs [13]). Permeability anisotropy can be estimated if the probe measurements are taken on slabs cut in different orientations.
Probe Acoustics	High resolution *p*- and *s*-wave transit times, and porosity profiles. Measurements can be made in different orientations in order to identify and quantify acoustic anisotropy (e.g., in 2D on the flat face of slabbed core). All these applications are relevant to hydrocarbon and energy transition reservoirs.
Probe Magnetic Susceptibility	Particularly useful for geothermal studies where identification of crystalline basement igneous and/or metamorphic rocks is important (where the magnetic susceptibility signals are high, and where many of the main heat producing minerals reside, compared to the much lower magnetic susceptibility signals of the sedimentary cover rocks). Applications for high resolution lithology discrimination, quantifying mineral content, and permeability prediction in turbidites, shales and oil sands have also been demonstrated [11, 12].